Electrochemistry Communications 115 (2020) 106730

Contents lists available at ScienceDirect

Electrochemistry Communications

journal homepage: www.elsevier.com/locate/elecom

# A scanning electrochemical microscopy (SECM) study of the interfacial solution chemistry at polarised chalcopyrite ($CuFeS_2$) and chalcocite ($Cu_2S$)

Rahul Ram[a,b], Victoria E. Coyle[a], Alan M. Bond[c], Miao Chen[a], Suresh K. Bhargava[a], Lathe A. Jones[a,*]

[a] Centre for Advanced Materials and Industrial Chemistry (CAMIC), School of Science, RMIT University, Melbourne, VIC 3001, Australia
[b] School of Earth, Atmosphere and Environment, Monash University, Clayton, VIC 3800, Australia
[c] School of Chemistry, Monash University, Clayton, VIC 3800, Australia

ARTICLE INFO

*Keywords:*
Chalcopyrite
SECM
Passivation
Copper

ABSTRACT

Chalcopyrite ($CuFeS_2$) passivation during hydrometallurgical copper extraction is attributed to multiple competing mechanisms that are still not completely understood. Here we have studied the interfacial solution chemistry *in situ* at polarised chalcopyrite and chalcocite, using scanning electrochemical microscopy (SECM). It was observed that the copper species detected at an ultramicroelectrode (UME) positioned at the mineral:solution interface vary between the two minerals, and are dependent upon both the potential of the mineral and the polarisation time. Cu species formed in the presence of sulfide, derived from incomplete oxidation of chalcopyrite, are observed on the UME tip positioned above chalcopyrite under conditions where passivation may occur, in contrast to Cu(II) in the presence of sulfate under conditions where leaching is facile. Only Cu(II) in the presence of sulfate is observed at the interface of chalcocite. These observations via interfacial voltammetry provide experimental support to mechanistic studies on chalcopyrite leaching, and provide new information to complement previous *in situ* studies which have mostly focused on interfacial solids.

## 1. Introduction

Hydrometallurgical leaching of metals from natural ores are usually redox processes involving oxidation of a solid-state mineral to dissolved ionic species, and are thus amenable to study *via* electrochemical methods [1–4]. Chalcopyrite ($CuFeS_2$) will be the most important copper mineral worldwide in coming decades due its presence in low grade ores [5–8], but can suffer from slow or incomplete extraction due to the formation of passivating layers at the solid–liquid interface. Passivation tends to be more pronounced at low temperature or high pH, and has been extensively studied using traditional electrochemical techniques with either bulk chalcopyrite or carbon paste electrodes [1–4]. Recent passivation studies have probed the surface of chalcopyrite either *ex situ* or *in situ* to detect the surface-based intermediates responsible, identifying species such as elemental sulfur or metal depleted species at the interface under passivating conditions [9–13]. A missing piece of the puzzle is an understanding of the solution chemistry at the interface. This information is not directly accessible through traditional electrochemical techniques when the chalcopyrite is the working electrode, nor is it picked up by common *in situ* techniques which tend to focus on transient solids formed on the surface of the chalcopyrite *via* techniques such as Raman spectroscopy or XRD [2,10,14].

In a heap leach which is typically used to process low-grade ores, the leaching of copper from $CuFeS_2$ is proposed to proceed by Eqs. (1) and (2).

$$CuFeS_2 + O_2 + 2H_2SO_4 \rightarrow CuSO_4 + FeSO_4 + 2S^0 + 2H_2O \quad (1)$$

$$CuFeS_2 + 2Fe_2(SO_4)_3 \rightarrow CuSO_4 + 5FeSO_4 + 2S^0 \quad (2)$$

At low potential, or after chalcopyrite has passed some time at the adopted corrosion potential, these equations become far more complicated, with various alternative copper or iron based species likely to be dissolved or precipitated on the surface, and elemental sulfur more likely to be formed as oxidation to soluble sulfates becomes incomplete [8]. In electrochemical studies the ferric-sulfate oxidizing agent, or oxygen, in Eqs. (1) and (2) are replaced by an electrode potential ($E_{cpy}$), where the $CuFeS_2$ is polarized anodically to facilitate dissolution, and potentiodynamic scans or potentiostatic experiments have been used to study chalcopyrite behavior [1–4].

Scanning electrochemical microscopy (SECM) in substrate generation–tip collection (SG–TC) mode allows the positioning of an

* Corresponding author.
*E-mail address:* lathe.jones@rmit.edu.au (L.A. Jones).

https://doi.org/10.1016/j.elecom.2020.106730
Received 7 February 2020; Received in revised form 9 April 2020; Accepted 9 April 2020
Available online 13 April 2020

ultramicroelectrode (UME) above a polarised substrate to probe the interfacial solution chemistry [15–19]. In this case parameters such as chalcopyrite potential, pH and temperature can be varied and the interfacial solution chemistry at a tip probed via electrochemical methods. The spatial resolution of SECM may allow the identification of solution-based markers where passivation predominates, and provide new information not previously seen by other methods commonly used *in situ*. In this communication we directly probe, for the first time, variations in copper interfacial chemistry at polarised copper minerals (chalcocite and chalcopyrite), providing evidence through copper species detected on the SECM tip, that the solution chemistry varies as a function of potential and polarisation time, and may act as a marker for hampered dissolution in refractory minerals such as chalcopyrite.

## 2. Experimental method

A natural chalcopyrite sample from Mt. Lyell in Tasmania (Australia), was set and polished into resin binder with a soldered pure copper wire (0.4 mm) as a contact to the back. A freshly polished mineral surface was used as a substrate electrode for each experiment, and Kapton film was used to isolate a geometric surface area of 7.1 $mm^2$ exposed to the solution. This chalcopyrite block electrode was used as the substrate, and polarized to a potential designated $E_{cpy}$. A 50 μm Pt UME was used as a tip, and was positioned approximately 100 μm above the chalcopyrite surface, using standard methods for surface approach with a ferrocenemethanol mediator solution while the chalcopyrite substrate was polarized at 0.2 V to ensure positive feedback [30,31], and was later flushed with $H_2SO_4$ solution before each SECM experiment. Voltammetry was undertaken with this tip ($E_{tip}$). SECM studies were undertaken in substrate generation–tip collection (SG–TC) mode, where the chalcopyrite substrate was held at constant potential with a CH Instruments CH920D potentiostat/SECM to construct a potentiostatic curve, or to simultaneously collect voltammetric data on the Pt tip. All experiments were conducted under a $N_2$ atmosphere in $N_2$ purged solution. A Pt wire counter electrode and Ag/AgCl reference electrode (3M NaCl, 0.210 V vs SHE) was used and corrected to SHE at 20°C.

## 3. Results and discussion

In the first step of this work, potentiostatic curves with chalcopyrite solid electrodes were collected, where the electrode potential ($E_{cpy}$) was controlled to mimic the corrosion potential of chalcopyrite during solution-based leaching [4,20]. These curves act as a starting point for the technique developed in this paper that will allow specific values of $E_{cpy}$ to be chosen for positioning of the UME at the interface. Potentiostatic (*i–t*) experiments on solid chalcopyrite at a range of $E_{cpy}$ led to the *i*–$E_{cpy}$ curves shown in Fig. 1 at four pH values at 20°C. The current–time profiles at each $E_{cpy}$ had stabilized after ~ 600 s, and this stable current is plotted in Fig. 1. The results showed a general increase in current with increasing $E_{cpy}$, with three regions identified on the potentiostatic curves, which include the passive (green), and transpassive (blue) regions. The drop in current in the passive region is seen to be more pronounced at the higher pH of 1.8, which is a trend commonly observed for chalcopyrite potentiostatic curves [4], and is indicative of the formation of surface passivating species.

Based on these potentiostatic curves, SG–TC studies were conducted to probe the solution chemistry at the interface. $E_{cpy}$ values of 0.72 V, 0.76 V and 0.80 V vs SHE were chosen for the chalcopyrite, with a 50 μm Pt UME tip positioned 100 μm above the chalcopyrite surface. A voltammetric profile of the interfacial solution was collected by scanning the tip potential ($E_{tip}$), enabling a study of the solution chemistry of redox active species released to the interface.

Fig. 2 displays the voltammetric profiles at the SECM tip (2B, C and D), at the three $E_{cpy}$ substrate potentials marked in Fig. 2A. It can be observed that four prominent anodic peaks can be identified and are

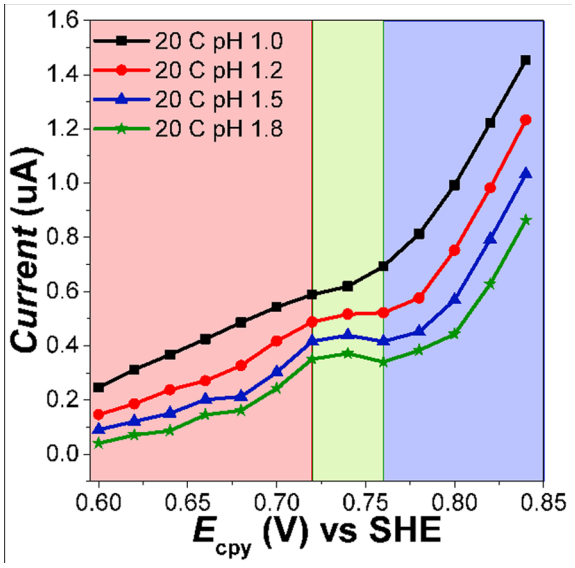


**Fig. 1.** Potentiostatic curves (*i*–$E_{cpy}$) of chalcopyrite block substrates at pH values 1.0, 1.2, 1.5 and 1.8 (20 °C). Each data point is the stable current after 600 s of an *i–t* potentiostatic experiment.

labelled a1, a2, a3 and a4. Cathodic processes are generally broad, with the most pronounced in Fig. 2D where the current is much higher, labelled c1. The well-known voltammetric signature of the Pt tip due to surface oxidation and H adatom adsorption/desorption in sulfuric acid is the baseline for these curves, and such features are labelled "Pt", and the baseline curve is shown in Fig. 2B (dotted line) [21]. In Fig. 2B ($E_{cpy}$ = 0.72 V vs SHE), the peaks a1 and a2 (small) are the main features apart from the Pt electrode background, as well as a cathodic response just above the baseline (c1), and thus represents the limit of the technique under these conditions to detect solution species, as the peaks assignable to copper species are just above the baseline (see Fig. 2B). A closer tip–substrate distance increases the sensitivity due to the enhanced concentration gradient, and the 100 μm tip–substrate distance was found to be the most repeatable substrate–tip separation with the 50 μm tip.

In assigning the peaks observed in the tip voltammograms, we need to consider the possible species that may be released, based on Fe and Cu ions in the presence of either sulfate, or sulfur-based compounds due to incomplete oxidation that may thus act as ligands.

In the transpassive region (Fig. 2D, $E_{cpy}$ = 0.80 V vs SHE), the profile is better defined, as the current at the tip increases relative to the background. a1 stabilizes to a peak shape typical of Cu stripping, another small peak arises (a2), and a3 appears, a peak with a symmetrical shape indicative of a surface bound copper species. In order to assign these peaks, voltammograms of standard solutions at the same Pt UME tip are given in Fig. 3A and B. Fig. 3B shows the voltammograms for $Cu^{2+}$ and $Fe^{2+}$ in $H_2SO_4$. It is observed that a1 is present for free $Cu^{2+}$, uncoordinated to any other species (sulfate is a weak ligand), and is in fact the expected response for deposition and stripping of copper in aqueous solution [22], while $Fe^{2+}$ shows a broad oxidation peak for the ferrous/ferric couple labelled as a4 [23,24]. In the presence of sulfur (Fig. 3A), the peaks a2 and a3 arise, and we can propose a3 is thus due to the deposition of copper in the presence of sulfide in solution, due to incomplete oxidation of chalcopyrite, leading to an anodic shift in the stripping potential [25–28]. This becomes the dominant peak in the presence of excess sulfide (see Fig. 3A (red)). The profile in Fig. 2D thus demonstrates the presence in solution of sulfur that has not been completely oxidized to sulfate, which leads to deposition of a copper-based species from solution onto the SECM tip. This peak (a3) is shifted to an anodic potential relative to free copper, followed at higher potential by the anodic peak (a4) due to $Fe^{2+}$ oxidation to $Fe^{3+}$. Fig. 3B

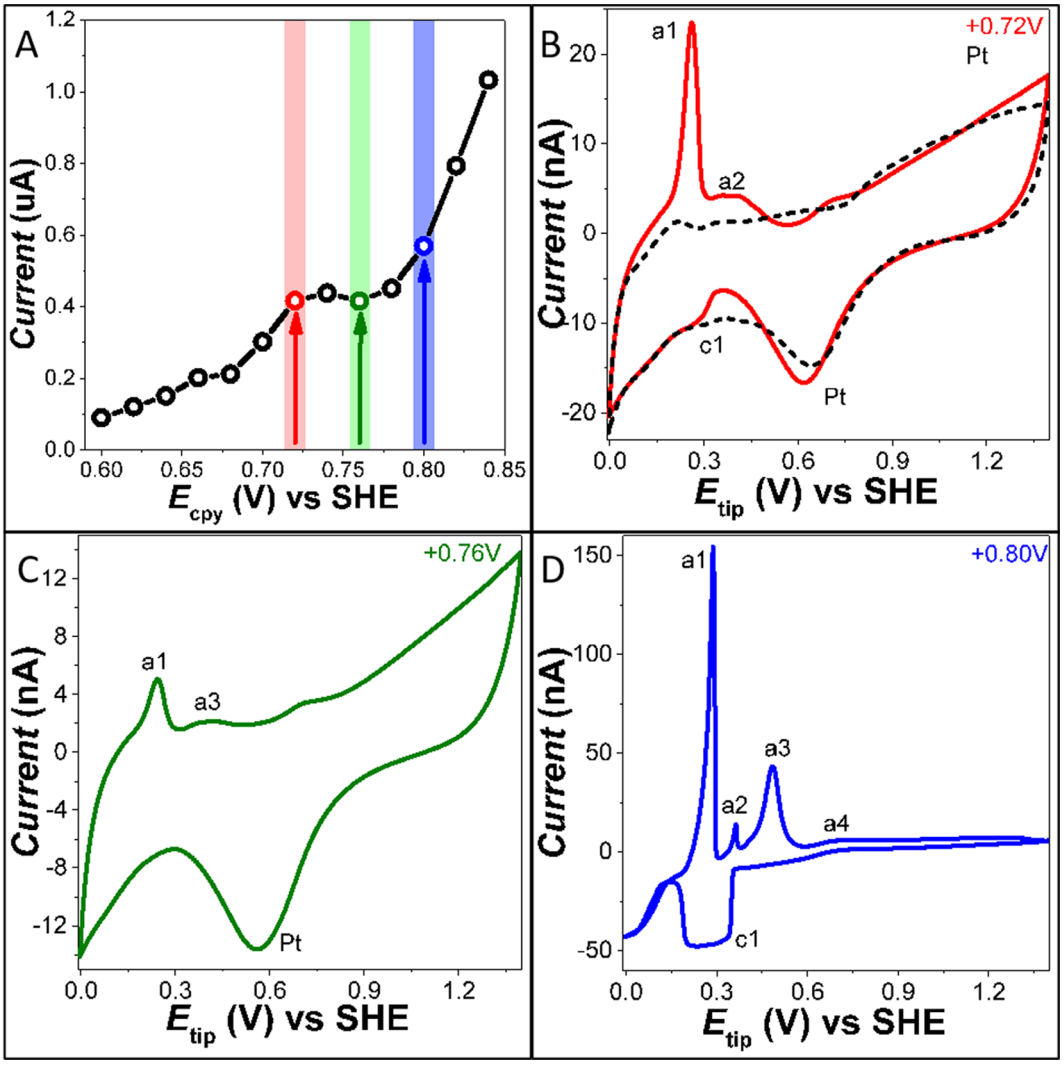


**Fig. 2.** a) Bulk potentiostatic *i–E* curve, and corresponding voltammograms at the UME tip during substrate generation–tip collection (SG–TC) scans, one minute after polarisation of chalcopyrite at pH 1.5, 20 °C held at $E_{cpy}$ values of b) 0.72 V, c) 0.76 V, and d) 0.80 V. Dotted line in 2B is the baseline of the Pt tip in $H_2SO_4$.

confirms that the voltammetry of the solution soluble $Fe^{2+/3+}$ couple at a microelectrode in aqueous sulfate solution [22] is of a sigmoidal shape (a4), and is sufficiently separated from the relatively sharp Cu stripping peak (a1), allowing discrimination between Fe and Cu based species released by chalcopyrite to the interface.

It has been previously established that the presence of sulfur species in solution may stabilize Cu(I) [25–29], and Cu(I) solution species may be present at the interface, however peak a3 can be considered, based on this evidence, as a marker for the presence of sulfide at the interface in the presence of either Cu(I) or Cu(II).

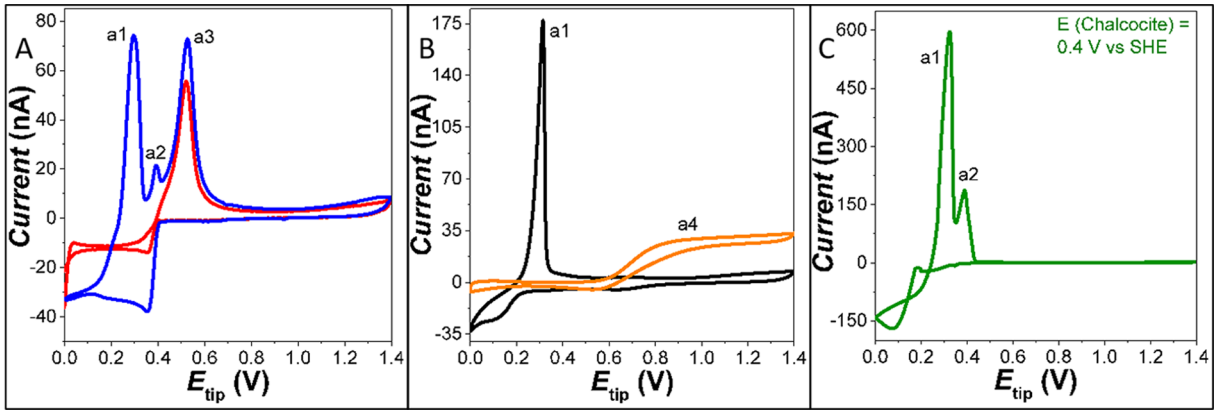


**Fig. 3.** A) Solution voltammetry at a Pt tip, containing 2:1 (blue) and 1:1 (red) stoichiometries of $Cu^{2+}$:$Na_2S$. b) Solution voltammetry at a Pt tip of $Cu^{2+}$ (black, showing a1) and $Fe^{2+}$ (orange, showing a4). C. SG–TC tip voltammetry at the interface of chalcocite at $E_{Chalcocite}$ = 0.4 V vs SHE. (For interpretation of the references to colour in this figure legend, the reader is referred to the web version of this article.)

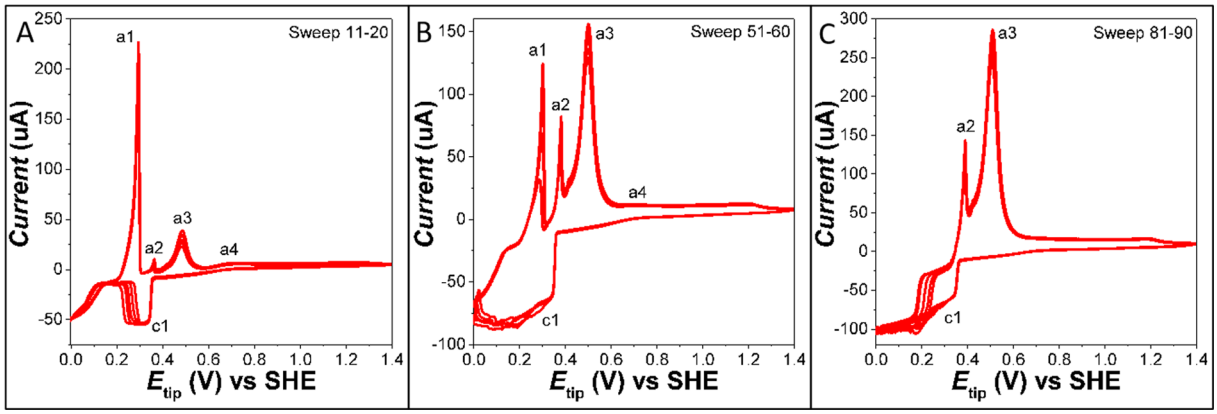


**Fig. 4.** Voltammograms at the UME tip at $E_{cpy}$ of 0.84 V vs SHE, as a function of time.

For comparison, an identical SG–TC SECM experiment with chalcocite ($Cu_2S$) was undertaken, and is shown in Fig. 3C. Of particular note is the low anodic potential $E_{Chalcocite}$ of 0.4 V, far lower than the chalcopyrite experiments, giving rise to peaks a1 and a2, which we can assign to copper stripping in the presence of sulfate, with a lack of any significant species due to sulfide in solution (i.e. peak a3 is absent). Chalcocite is not a refractory mineral, and does not passivate as chalcopyrite does during leaching, and this is confirmation that the interfacial solution chemistry of the chalcocite is devoid of sulfide or sulfur coordinated species. The peak a3 may thus be considered a marker for conditions that lead to passivation.

Fig. 4 shows tip voltammograms for polarised chalcopyrite after a larger number of sweep segments, in order to study the variations of interfacial chemistry with time at $E_{cpy}$ = 0.84 V. Each scan lasts for one minute, so the profile in Fig. 4C corresponds to a polarisation window of 80–90 min. It can be observed in these scans that interfacial chemistry changes over time. As evidenced in Sweeps 1–10, the dominant peak is a1, and as the time progresses in Fig. 4B and C, peak a3, assigned above to copper in the presence of a sulfur species such as sulfide, becomes more dominant.

This transition from peaks a1 and a2 to a3 over time is indicative of evolving mechanisms on the surface of the chalcopyrite. In this case, as the surface is polarised over more than one hour, sulfur species are observed at the interface to a greater extent. The positioning of the electrode at different distances above the chalcopyrite substrate did not affect these voltammetry profiles, indicating that the change is not due to a variable tip–substrate distance due to dissolution. Peak a3 may thus be assigned to a copper species deposited on the tip in the presence of sulfide in solution, and can be considered as a solution-based marker for surface passivation of chalcopyrite due to incomplete oxidation.

## 4. Conclusion

Scanning electrochemical microscopy in substrate generation–tip collection mode has been successfully used to contrast the interfacial solution chemistry of two copper minerals, chalcopyrite and chalcocite. This technique reveals that incomplete oxidation of the economically important chalcopyrite mineral can be directly observed using a solution-based marker, especially through an anodic peak that is deposited on the UME when copper is in the presence of sulfide, a species that increases with polarisation time. Resolution of copper from iron species was possible due to separation of the anodic responses at higher solution concentrations. Metal deficient surface species generated during chalcopyrite polarisation that have been observed with other surface characterisation techniques will now be able to take into account these interfacial solution species. Further follow-on studies at a range of conditions will allow elucidation of solution species of copper and iron in solution at the interface, and identification of the copper species deposited on the tip. This technique and initial results complement other studies on chalcopyrite leaching mechanisms which have mostly revealed solids formed at the interface during chalcopyrite polarisation, with limited information previously obtained on species in solution.

## CRediT authorship contribution statement

**Rahul Ram:** Investigation, Methodology, Formal analysis, Writing - review & editing. **Victoria E. Coyle:** Investigation, Formal analysis, Writing - review & editing. **Alan M. Bond:** Formal analysis, Writing - review & editing. **Miao Chen:** Writing - review & editing. **Suresh K. Bhargava:** Writing - review & editing. **Lathe A. Jones:** Conceptualization, Methodology, Investigation, Writing - original draft.

## Declaration of Competing Interest

The authors declare that they have no known competing financial interests or personal relationships that could have appeared to influence the work reported in this paper.

## Acknowledgements

We acknowledge funding from the Australian Research Council (LP13010091).

## References

[1] G. Debernardi, C. Carlesi, Chemical-electrochemical approaches to the study passivation of chalcopyrite, Miner. Process. Extr. Metall. Rev. 34 (2013) 10–41.
[2] D. Majuste, V.S.T. Ciminelli, K. Osseo-Asare, M.S.S. Dantas, R. Magalhães-Paniago, Electrochemical dissolution of chalcopyrite: detection of bornite by synchrotron small angle X-ray diffraction and its correlation with the hindered dissolution process, Hydrometallurgy 111–112 (2012) 114–123.
[3] B.R. Vasquez, G.V. Gamboa, D.G. Dixon, Transpassive electrochemistry of chalcopyrite microparticles, J. Electrochem. Soc. 159 (2012) C8–C14.
[4] G. Viramontes-Gamboa, M.M. Pena-Gomar, D.G. Dixon, Electrochemical hysteresis and bistability in chalcopyrite passivation, Hydrometallurgy 105 (2010) 140–147.
[5] Y. Li, N. Kawashima, J. Li, A.P. Chandra, A.R. Gerson, A review of the structure, and fundamental mechanisms and kinetics of the leaching of chalcopyrite, Adv. Colloid Interface Sci. 197–198 (2013) 1–32.
[6] R. Ram, L. Beiza, M. Becker, M.I. Pownceby, M. Chen, Y. Yang, S. Yang, J. Petersen, Study of the leaching and pore evolution in large particles of a sulfide ore, Hydrometallurgy 105261 (2020).
[7] M.C. Ruiz, K.S. Montes, R. Padilla, Chalcopyrite leaching in sulfate–chloride media at ambient pressure, Hydrometallurgy 109 (2011) 37–42.
[8] H. Zhao, Y. Zhang, X. Zhang, L. Qian, M. Sun, Y. Yang, Y. Zhang, J. Wang, H. Kim, G. Qiu, The dissolution and passivation mechanism of chalcopyrite in bioleaching: an overview, Miner. Eng. 136 (2019) 140–154.
[9] G.F. de Lima, H.A. Duarte, L.G. Pettersson, X-ray absorption near-edge spectroscopy calculations on pristine and modified chalcopyrite surfaces, J. Phys. Chem. C 122 (2018) 20200–20209.
[10] D. Majuste, V.S.T. Ciminelli, P.J. Eng, K. Osseo-Asare, Applications of in situ synchrotron XRD in hydrometallurgy: literature review and investigation of

chalcopyrite dissolution, Hydrometallurgy 131–132 (2013) 54–66.
[11] V. Nasluzov, A. Shor, A. Romanchenko, Y. Tomashevich, Y. Mikhlin, DFT + *U* and low-temperature XPS studies of Fe-depleted chalcopyrite ($CuFeS_2$) surfaces: a focus on polysulfide species, J. Phys. Chem. C 123 (2019) 21031–21041.
[12] K. Sasaki, Y. Nakamuta, T. Hirajima, O. Tuovinen, Raman characterization of secondary minerals formed during chalcopyrite leaching with *Acidithiobacillus ferrooxidans*, Hydrometallurgy 95 (2009) 153–158.
[13] K. Sasaki, K. Takatsugi, K. Ishikura, T. Hirajima, Spectroscopic study on oxidative dissolution of chalcopyrite, enargite and tennantite at different pH values, Hydrometallurgy 100 (2010) 144–151.
[14] G.K. Parker, G.A. Hope, R. Woods, Gold-enhanced Raman observation of chalcopyrite leaching, Colloids Surf., A 325 (2008) 132–140.
[15] R. Cornut, S. Nunige, C. Lefrou, F. Kanoufi, Local etching of copper films by the Scanning Electrochemical Microscope in the feedback mode: a theoretical and experimental investigation, Electrochim. Acta 56 (2011) 10701–10707.
[16] P.M. Diakowski, M. Chen, Surface analysis of materials in aqueous solution by localized alternating current impedance measurements, Anal. Chem. 84 (2012) 7622–7625.
[17] H. He, R.K. Zhu, Z. Qin, P. Keech, Z. Ding, D.W. Shoesmith, Determination of local corrosion kinetics on hyper-stoichiometric $UO_{[2+x]}$ by scanning electrochemical microscopy, J. Electrochem. Soc. 156 (2009) C87–C94.
[18] R.M. Souto, S.V. Lamaka, S. Gonzalez, Uses of scanning electrochemical microscopy in corrosion research, in: A. Méndez-Vilas, J. Díaz (Eds.), Microscopy: Science, Technology, Applications and Education, Formatex (Spain), 2010, pp. 1769–1780.
[19] R.M. Souto, Y. González-García, D. Battistel, S. Daniele, In situ scanning electrochemical microscopy (SECM) detection of metal dissolution during zinc corrosion by means of mercury sphere-cap microelectrode tips, Chem.– Eur. J. 18 (2012) 230–236.
[20] B. Manana, J. Petersen, R. Ram, Study of the diffusion of Cu (II) as an oxidant through simulated particle pores in a novel model apparatus, in: Extraction 2018, Springer, 2018, pp. 1361–1372.
[21] D.A.J. Rand, R. Woods, A study of the dissolution of platinum, palladium, rhodium and gold electrodes in 1 *M* sulphuric acid by cyclic voltammetry, J. Electroanal. Chem. Interfacial Electrochem. 35 (1972) 209–218.
[22] B.D.B. Aaronson, C.H. Chen, H. Li, M.T.M. Koper, S.C.S. Lai, P.R. Unwin, Pseudo-single-crystal electrochemistry on polycrystalline electrodes: visualizing activity at grains and grain boundaries on platinum for the $Fe^{2+}/Fe^{3+}$ redox reaction, J. Am. Chem. Soc. 135 (2013) 3873–3880.
[23] K. Brainina, E. Neyman, Electroanalytical Stripping methods, in: J.D. Winefordner (Eds.), Chemical Analysis: A Series of Monographs on Analytical Chemistry and its Applications, Vol. 126, John Wiley & Sons, 1994.
[24] Y. Bonfil, M. Brand, E. Kirowa-Eisner, Determination of sub-μg $l^{-1}$ concentrations of copper by anodic stripping voltammetry at the gold electrode, Anal. Chim. Acta 387 (1999) 85–95.
[25] A. Carreon-Alvarez, N. Casillas, J.G. Ibanez, F. Hernandez, R. Prado-Ramírez, M. Barcena-Soto, S. Gómez-Salazar, Determination of Cu in tequila by anodic stripping voltammetry, Anal. Lett. 41 (2008) 469–477.
[26] L.M. Laglera, C.M.G. van den Berg, Copper complexation by thiol compounds in estuarine waters, Mar. Chem. 82 (2003) 71–89.
[27] G.W. Luther, D.T. Rickard, S. Theberge, A. Olroyd, Determination of metal (bi) sulfide stability constants of $Mn^{2+}$, $Fe^{2+}$, $Co^{2+}$, $Ni^{2+}$, $Cu^{2+}$, and $Zn^{2+}$ by voltammetric methods, Environ. Sci. Technol. 30 (1996) 671–679.
[28] T.F. Rozan, G. Benoit, G.W. Luther, Measuring metal sulfide complexes in oxic river waters with square wave voltammetry, Environ. Sci. Technol. 33 (1999) 3021–3026.
[29] K. Sukola, F. Wang, A. Tessier, Metal-sulfide species in oxic waters, Anal. Chim. Acta 528 (2005) 183–195.
[30] G. Liu, Z. Qiu, J. Wang, Q. Liu, J. Xiao, H. Zeng, H. Zhong, Z. Xu, Study of N-isopropoxypropyl-N′-ethoxycarbonyl thiourea adsorption on chalcopyrite using in situ SECM, ToF-SIMS and XPS, J. Colloid Interface Sci. 437 (2015) 42–49.
[31] J. Xiao, N. Di, G. Liu, H. Zhong, The interaction of N-butoxypropyl-N′-ethoxycarbonylthiourea with sulfide minerals: scanning electrochemical microscopy, diffuse reflectance infrared Fourier transform spectroscopy, and thermodynamics, Colloids Surf., A 456 (2014) 203–210.